A Conserved Electrostatic Membrane-Binding Surface in Synaptotagmin-Like Proteins Revealed Using Molecular Phylogenetic Analysis and Homology Modeling

Nara L. Chon[1], Sherleen Tran[1], Christopher S. Miller[2], Hai Lin[1], and Jefferson D. Knight[1]

[1] Department of Chemistry, University of Colorado Denver

[2] Department of Integrative Biology, University of Colorado Denver

Corresponding author: Jefferson D. Knight, Campus Box 194, PO Box 173364, Denver, CO 80217-3364 USA. Tel: +1 303 315 7639. Fax: +1 303 315 7633. Email: Jefferson.Knight@ucdenver.edu

Running title: Evolutionary analysis of Slp electrostatics

Total manuscript pages: 33. Supplementary material pages: 5. Tables: 0. Figures: 8.

Description of Supplementary Material: PDF file containing Figures S1-S3 and Table S1; Spreadsheet file and FASTA file listing all Slp-4 sequence clusters analyzed; Zip file containing 9 homology-generated protein structure PDB files.

Abstract

Protein structure prediction has emerged as a core technology for understanding biomolecules and their interactions. Here, we combine homology-based structure prediction with molecular phylogenetic analysis to study the evolution of electrostatic membrane binding among vertebrate synaptotagmin-like proteins (Slps). Slp family proteins play key roles in the membrane trafficking of large dense-core secretory vesicles. Our previous experimental and computational study found that the C2A domain of Slp-4 (also called granuphilin) binds with high affinity to anionic phospholipids in the cytoplasmic leaflet of the plasma membrane through a large electropositive protein surface centered on a cluster of phosphoinositide-binding lysine residues. Because the polybasic surface contributes greatly to Slp-4 C2A domain membrane binding, we hypothesized that the net charge on the large electropositive surface might be evolutionarily conserved. To test this hypothesis, the known C2A sequences of Slp-4 among vertebrates were organized by class (from mammalia to pisces) using molecular phylogenetic analysis. Consensus sequences for each class were then identified and used to generate homology structures, from which Poisson–Boltzmann electrostatic potentials were calculated. For comparison, homology structures and electrostatic potentials were also calculated for the five human Slp protein family members. The results demonstrate that the charge on the membrane-binding surface is highly conserved throughout the evolution of Slp-4, and more highly conserved than many individual residues in the mammalian Slp C2A domain family overall. Such molecular phylogenetic-driven computational analysis can help to describe the evolution of electrostatic interactions between proteins and membranes which are crucial for their function.

Keywords: synaptotagmin-like, SytL, Syt, rabphilin, Poisson-Boltzmann, electrostatics, basic protein, evolution, homology modeling

Impact statement:

The interior surface of eukaryotic plasma membranes is negatively charged, and many proteins that bind to this surface have correspondingly evolved a positively charged face. Here, we use techniques from evolutionary biology and computational biophysics to study the conservation of this electropositive surface among one family of proteins. We find that the overall surface charge is highly conserved, more so than individual amino acids, consistent with its important role in electrostatic interaction with the membrane.

Introduction

Membrane-targeting protein domains play many key roles in biology, particularly within eukaryotic secretory pathways. Distributed among several evolutionarily conserved families including C2, PX, and pleckstrin homology (PH) domains, membrane-targeting protein domains are normally soluble in the cytoplasm and drive binding to membrane surfaces in response to signaling events (Lemmon 2008). Typical biochemical signals that proteins recognize include phosphoinositide lipid species and/or Ca^{2+} ions (Corbalan-Garcia & Gomez-Fernandez 2014). In addition, many membrane-binding protein domains also interact with lipid bilayers via nonspecific interactions such as insertion of hydrophobic sidechains into the membrane interior and electrostatic attraction of lysine and arginine residues to anionic phospholipid headgroups (Lemmon 2008). Electrostatic interactions are arguably the most important type of interaction between peripheral proteins and membranes. They are especially important for protein binding to the plasma membrane inner leaflet, which contains approximately 20% phosphatidylserine (PS), 5% phosphatidylinositol (PI), and 1-2% phosphatidylinositol-(4,5)-bisphosphate (PIP2) (Murray & Honig 2002; Voelker 2008). While some interactions with phosphoinositides are highly specific, nonspecific electrostatic interactions also play key roles in membrane targeting and increasing affinity. How membrane-binding protein surfaces have evolved to optimize both specific and nonspecific electrostatic interactions with lipid membranes is a subject that has not been extensively explored.

Here, we chose to use C2A domains from the synaptotagmin-like protein (Slp) family as a model system to explore the evolutionary conservation of the membrane-binding face, which includes a PIP2-binding motif in the center of a large polybasic surface. Discovered in the early 2000s, the Slp family consists of five proteins conserved throughout vertebrates; at least one is

also present in invertebrates (Serano & Rubin 2003). The Slp family is structurally related to synaptotagmins but lack synaptotagmins' Ca^{2+}-dependent membrane fusion capability (Wang et al. 1999; M. Fukuda & Mikoshiba 2001; M. Fukuda 2013; Bhalla et al. 2008). Rather, Slp proteins are Rab27 effectors that function to dock large dense-core secretory vesicles to the plasma membrane prior to exocytosis in a variety of cell types (T. S. Kuroda et al. 2002; M. Fukuda 2013; Izumi 2021). Because Slp family proteins can inhibit exocytosis prior to Ca^{2+} entry, understanding their mechanisms of membrane interaction may be important for understanding secretory pathways and their dysfunction in diseases such as diabetes (Tomas et al. 2008; Tsuboi 2009; Izumi 2011). All Slp proteins contain an N-terminal Slp homology domain (SHD) capable of binding Rab GTPases on secretory granules (Fukuda et al. 2001; Chavas et al. 2008), as well as two C-terminal C2 domains, termed C2A and C2B.

Originally named from the second conserved domain in protein kinase C (PKC), C2 domains are the 2nd-most abundant family of conserved protein domains and are found in over 120 mammalian proteins (Nalefski & Falke 1996; Cho & Stahelin 2006; Corbalan-Garcia & Gomez-Fernandez 2014). Several subfamilies of C2 domains have been identified, among which only the PKC type has members that bind membranes in response to Ca^{2+} (D. Zhang & Aravind 2010). Several secretory pathway proteins contain two or more C2 domains, including synaptotagmins, Slp proteins, double-C2 (Doc2) proteins, rabphilins, Munc13, ferlins, RIM proteins, and others (Cho & Stahelin 2006; Corbalan-Garcia & Gomez-Fernandez 2014; Dominguez et al. 2022). Some well-known PKC-type C2 domains, such as those from PKC-α and synaptotagmin-1, bind anionic membranes in response to Ca^{2+} influx (Brose et al. 1992; Sutton et al. 1995; Edwards & Newton 1997). These C2 domains bind one to three Ca^{2+} ions through a conserved set of five anionic residues, typically aspartates (Nalefski & Falke 1996;

Murray & Honig 2002). Others lack a full complement of these aspartates but bind membranes containing anionic lipids even in the absence of Ca^{2+} (Yi et al. 2002). A consensus sequence for binding the plasma membrane lipid PIP2, including a cluster of three lysine residues, has been recognized among some PKC-type C2 domains, including both Ca^{2+}-dependent and Ca^{2+}-independent proteins (Guerrero-Valero et al. 2009; Corbalan-Garcia & Gomez-Fernandez 2014). This PIP2-binding consensus sequence has been observed in Slp family proteins, which typically do not require Ca^{2+} for binding membranes (Galvez-Santisteban et al. 2012; Alnaas et al. 2021). [We note, however, that Ca^{2+} is reported to enhance membrane binding of the Slp-3 and Slp-5 C2A domains (M. Fukuda 2002; Taruho S. Kuroda et al. 2002) and to inhibit Slp-2 C2 domains (Yu et al. 2007); the underlying mechanisms have not been fully described.]

The best-studied Slp family member, Slp-4 (also known as granuphilin), is a key factor in insulin secretion (Izumi et al. 2007; Yamaoka et al. 2015). Previous studies from our lab and others showed that the C2A domain of human Slp-4 binds physiological membranes with high affinity through nearly equal contributions of (i) the conserved PIP_2-binding lysine cluster and (ii) a large polybasic surface (Yu et al. 2007; Lyakhova & Knight 2014; Wan et al. 2015; Alnaas et al. 2021). Mutation of individual residues on the large polybasic surface has little effect on membrane binding affinity, suggesting the attraction is mainly electrostatic and nonspecific; it is also strong enough to drive membrane binding even in the absence of phosphoinositides (Alnaas et al. 2021). In light of this mechanism involving both PIP2-selective binding and strong nonspecific binding of background anionic lipids, we set out to explore the evolutionary conservation of the positive charges on this surface.

The goal of the current study is to determine the level of conservation of the large electropositive surface on the C2A domain of Slp-4 and the broader Slp family. We hypothesized

that the surface surrounding the PIP2-binding pocket evolved to bind membranes containing anionic background lipids with high affinity but low specificity; if so, then the overall charge of the surface might be more highly conserved than individual basic residues. Thus, we compiled the known sequences of C2A domains from vertebrate Slp-4 proteins and the other human Slp family members, predicted structures from consensus sequences, and compared conservation both at the sequence level and among the calculated electrostatic surface potentials.

Results

Strategy

The C2A domain of Slp-4 is the only Slp family C2 domain with a published experimental structure (PDB: 3FDW). Its PIP2-binding consensus sequence is centered on a triad of lysine residues in the β_3 and β_4 strands while the broad electropositive surface surrounding this site includes residues from throughout the C2 domain sequence (Wan et al. 2015; Alnaas et al. 2021). In order to test the extent of conservation in this nonspecific electrostatic surface, we performed a phylogenetic alignment of Slp-4 C2A domains across vertebrates, extracted consensus sequences, and used homology modeling to construct structures. Although homology modeling has limitations, the level of homology among Slp family proteins is high, inspiring good confidence in the generated structures including the electropositive membrane binding surfaces. From these structures, we calculated electrostatic surface maps to visualize the charge distribution on the protein surface. Because the vertebrate Slp-4 C2A domains showed a high level of conservation of individual membrane-binding residues and the electropositive surface, we also compared electrostatic surface potentials among homology model structures of C2A domains from the five human Slp family members.

Conservation in Slp-4 primary structure

Amino acid sequence comparisons reveal a high conservation of membrane-binding residues on Slp-4 C2A domains. Using the Uniref90 database, we identified 218 Slp-4 C2A domain sequences (Uniref90 cluster representatives) with at least 50% identity to human Slp-4, spanning the subphylum vertebrata from fish to mammals. (Sequences in the database with

<50% identity tended to align more closely with human Slp-5 than Slp-4; therefore, we only analyzed sequences with > 50% identity to human Slp-4.) A phylogeny of these sequences shows that the sequences cluster by taxonomic class, as expected (**Figure 1A**), with clear clusters for mammals, birds, amphibians, reptiles, and fishes. The predicted net charges on these protein domain sequences tend to decrease as the level of identity with the human sequence decreases, with the lowest average net charge among the class pisces (**Figure 1B; Table S1**). Interestingly, the trend in net positive charge tended to correlate with the number of lysine residues, while the average count of arginine residues remained relatively constant among the different classes (**Table S1**). Overall, all of the Slp-4 C2A sequences maintain a predicted positive net charge.

From each taxonomic class (mammalia, aves, reptilia, amphibia, and pisces), a consensus sequence was generated as described in Methods. An alignment of these consensus sequences is shown in **Figure 2**. The alignment shows complete conservation of the consensus PIP2 binding site found on many C2 domains, (Corbalan-Garcia & Gomez-Fernandez 2014) which consists of three lysine residues (Lys398, Lys410, and Lys412) along with nearby Tyr396, Trp447, and Asn455 on human Slp-4 (**Figure 2**, red boxes). (For consistency, we report all numbering based on the human Slp-4 sequence.)

Beyond the PIP2-binding pocket, our prior molecular dynamics simulations and mutagenesis experiments identified ten additional basic residues on Slp-4 that participate in nonspecific membrane binding and one hydrophobic sidechain that inserts into the nonpolar membrane interior (Alnaas et al. 2021). As shown in **Figure 2**, all of these basic residues maintain conserved charge among the consensus sequences except that Arg392 in human Slp-4 corresponds to a leucine in the pisces sequence, although we note that 33% of the pisces sequences contain Lys or Arg at this position. Similarly, the membrane-inserting residue Phe452

is conserved in all consensus sequences except pisces where it is the slightly less hydrophobic leucine. Thus, the membrane-binding residues of the Slp-4 C2A domain are well conserved at the sequence level.

Electrostatic surface maps show high conservation in Slp-4

The electrostatic surface of the Slp-4 C2A domain is highly conserved from fish to humans. We threaded each of the consensus sequences in **Figure 2** onto the published human Slp-4 C2A crystal structure using SwissModel (Waterhouse et al. 2018) and calculated electrostatic surfaces using APBS (**Figure 3**) (Baker et al. 2001). Strikingly, the membrane-binding polybasic surface (shown as a blue surface extending in the -z direction) is highly similar among all the classes of the protein. The volume of the electropositive surface is slightly smaller in fish, corresponding to the presence of leucine at position 392 instead of arginine. The charged surface on the region near Phe452 in the mammalian structure is greatly positive. However, some negative charge is visible in that region in the other classes. These small areas stem in part from the presence of an Asp at position 450 in most of the non-mammalian structures.

These differences in the electropositive membrane binding surface are much smaller than the electrostatic differences in the surface pointing away from the membrane (+z direction in **Figure 3**), which vary considerably among the different classes. Also at the primary sequence level, conservation in the +z surface is also lower than on the membrane-facing surface (**Figure S1**). Thus, the membrane-facing surface of this domain is highly conserved in both sequence and electrostatics.

In order to quantify the similarity in the electropositive surface, we used the webPIPSA tool which was developed for comparing electrostatic protein-protein interaction surfaces

(Richter et al. 2008). Focusing on the electropositive membrane-facing surface, we calculated similarity indices (SI) for the human and each class consensus structure versus every other class consensus structure (**Figure 4**). The full SI scale ranges from zero (identical) to 1.4 (uncorrelated) to 2.0 (fully anti-correlated). Slp-4 C2A pairs all had SI values of 0.33 or less, indicating strong correlation. Consistent with its visual appearance, the pisces Slp-4 C2A domain had the largest SI values when compared to the other consensus structures.

Despite this general agreement, a variability in local charge is visible near Phe452 on the membrane-facing region. This is the main reason why the mammalian Slp-4 is somewhat further from the other classes in the dendrogram along the top of **Figure 4**.

Electrostatic surface comparison among human Slp paralogs

The analysis above shows that the Slp-4 C2A membrane-binding surface is highly conserved both in sequence and electrostatics. If the electropositive membrane-binding surface is an evolutionarily conserved feature important for protein function, one prediction is that the overall electropositive character among the C2A domains of the larger family of synaptotagmin-like proteins may be more strongly conserved than individual residues. In order to test this prediction, we expanded our comparison to the sequences and predicted structures of all five human Slp C2A domains.

Some of the membrane-binding residues in Slp-4 C2A are conserved among Slp family proteins while others are not (**Figure 5**). Five of the six consensus residues for PIP2 binding are completely conserved, and the sixth (Asn455) is conserved in four of the five proteins. Of the ten additional membrane-binding basic residues we previously identified in Slp-4, five are

completely conserved as basic while the other five are not completely conserved. For the non-conserved residues, the proteins that lack a basic residue at that position sometimes have one nearby; for example, Slp-1 and Slp-2 lack an Arg at position 451 but contain an Arg at 449 that is not present in Slp-4.

Electrostatic surfaces of the homology model structures of human Slp-1 through Slp-5 show differences in the size and location of the electropositive surface, consistent with the sequence comparison (**Figure 6**). The electropositive lobe is largest in Slp-1 and Slp-2, is shifted toward the -y direction in Slp-1, and is smaller and shifted more toward the +y direction in Slp-5. However, strong electropositive character is clearly present on the -z surface of all five protein domains, whereas the electrostatics of the +z surfaces vary substantially among the five family members. Quantitative comparison using webPIPSA confirms that the similarities are relatively strong, with most SI values less than 0.5 (**Figure 7**). The domain with the least similarity to the others was Slp-5 with an average SI score of 0.45, while two pairs of structures (Slp-1/Slp-3 and Slp-3/Slp-4) had SI scores as low as 0.28 showing the greatest similarity. Notably, the conservation of electrostatic surface does not necessarily parallel evolution overall, as Slp-4 and Slp-5 are the two most closely related family members based on sequence analysis (Kuroda et al. 2002) Together, these results support the assertion that electrostatic membrane binding is an evolutionarily conserved feature of the Slp family C2A domains, as the presence of an electropositive surface is more strongly conserved than several of the individual basic residues on that surface.

Discussion

Importance of electrostatic surfaces

Proteins interact with lipid membrane surfaces through a combination of nonspecific electrostatic attractions, the hydrophobic effect, and specific molecular recognition. In particular, electrostatic attraction can contribute greatly toward overall binding affinity for a negatively charged membrane. In biological systems, both the affinity and the specificity of interactions are tuned to match the native environment. Coincidence detection is a common feature of peripheral protein-lipid interactions (Lemmon 2008), which allows for membrane specificity and affinity to be tuned via separate sites or regions of a protein. In vertebrates, nonspecific electrostatic attractions contribute not only to affinity through Coulombic attraction, but also to membrane specificity because the plasma membrane inner leaflet is enriched in anionic lipids relative to internal membranes such as ER and Golgi (Corbin et al. 2007; van Meer et al. 2008). Thus, investigating evolutionary conservation can offer clues as to the importance of electrostatics in protein-lipid interactions.

In this study, we have used phylogenetic analysis and structure prediction to compare the evolutionary conservation of a polybasic membrane-binding surface from C2A domains of Slp family proteins. These bind membranes through (1) a conserved PIP2 binding site; (2) a polybasic surface surrounding the PIP2 binding site; and (3) a single membrane-inserting hydrophobic residue. It is clear from simple sequence analysis that the PIP2-binding residues are highly conserved (**Figures 2 and 5**). Our electrostatic analysis further shows that the large polybasic surface is also a conserved feature of this family of proteins. Notably, the results indicate the overall surface charge on the membrane binding surface is more highly conserved

than several of the individual basic residues outside of the PIP2 binding site. Not surprisingly, individual basic residues are more highly conserved among vertebrate orthologs of Slp-4 than when comparing across human Slp family paralogs.

Sequence conservation among Slp proteins and relatives

Slp family proteins are closely evolutionarily related to synaptotagmins, rabphilins, and Doc2b proteins, all of which contain tandem C2 domains belonging to the protein kinase C-type family (PKC-C2) (M. Fukuda & Mikoshiba 2001; Rickman et al. 2004; Craxton 2010; D. Zhang & Aravind 2010; Tellez-Arreola et al. 2022). This family of C2 domains is typically characterized by Ca^{2+}-dependent membrane binding, and many but not all synaptotagmins as well as rabphilins and Doc2b C2 domains bind membranes in a Ca^{2+}-dependent manner (D. Zhang & Aravind 2010). The Ca^{2+}-dependent synaptotagmin C2 domains typically contain 5 conserved Asp residues in a Ca^{2+}-binding pocket: two in the β_2-β_3 loop and three in the β_6-β_7 loop (**Figure 8**). However, Slp family C2A domains lack most or all of these Asp residues: vertebrate Slp-4 consensus sequences contain one (mammalia, pisces) or two (aves, reptilia, amphibia) Asp residues at the calcium-binding positions, and the rest of the human Slp domains contain between zero (Slp-3) and three (Slp-2 and Slp-5) (**Figure 8**). This pattern is consistent with a functional loss of Ca^{2+} binding by Slp C2A domains after diverging from a common ancestor with synaptotagmins and other related proteins. Interestingly, Slp C2A domains contain a conserved His at one of these positions (H448 in human Slp-4) whose role is unknown. Its position at the base of the pocket suggests it could function as a pH sensor analogous to some PH domains (He et al. 2008) or to bind some other metal, although we note that our lab has not observed Zn^{2+} binding in tests with C2A domains of Slp-4 and Slp-2 (data not shown).

The Slp-4 C2A domain also contains a single membrane-inserting hydrophobic residue at the tip of its β_6-β_7 loop, corresponding to Phe452 in human Slp-4. This residue was Phe or Leu in all sequences analyzed in **Figure 2 and 5**. In contrast, C2A domains of membrane-binding synaptotagmins typically have a hydrophobic residue at this position plus another one on the β_2-β_3 loop (**Figure 8**) (X. Zhang et al. 1998; Osterberg et al. 2015). Among the Slp sequences analyzed, only human Slp-2 (Val) and pisces Slp-4 (Ala) had hydrophobic residues at this second position, suggesting that membrane insertion of the β_2-β_3 loop may be another feature that is being lost following divergence from the last common ancestor with synaptotagmins. In Slp C2A domains, the Phe or Leu on the β_6-β_7 loop is surrounded by a large lobe of positive charge (**Figures 3 and 6**), although the presence of Asp or Glu residues add small patches of negative charge nearby in some Slp-4 sequences (**Figure 3**) and human Slp-5 (**Figure 6**).

The conserved motif by which Slp C2A domains bind PIP2 is present in many C2B domains of synaptotagmins, but not the C2A domains of Ca^{2+}-dependent synaptotagmins (Guillen et al. 2013; Alnaas et al. 2021). To our knowledge, no evolutionary analysis of synaptotagmin electrostatic surfaces for synaptotagmins has been conducted, although electrostatic surface maps have been reported for some individual synaptotagmin C2 domains (Chon et al. 2015; MacDougall et al. 2018). It would be interesting to compare the level of conservation seen in the Slp polybasic surface to those of other subfamilies of C2 domains.

Usefulness of this approach to studying protein-membrane interactions

To our knowledge, this is the first study to combine evolutionary and structural modeling to study conservation of a membrane-binding electrostatic surface among a family of C2 domain proteins. Typical prior approaches address C2 domain evolutionary relationships at the sequence

level to determine key consensus motifs and/or identify new subfamilies of proteins (Craxton 2010; D. Zhang & Aravind 2010; Farrell et al. 2012; D. Zhang & Aravind 2012; Tellez-Arreola et al. 2022). Several studies have observed that Ca^{2+} switches the electrostatic profile of many C2 domains from negative to positive, beginning with the seminal work of Murray and Honig (Murray & Honig 2002). A more recent study has performed detailed molecular dynamics simulations of selected Ca^{2+}-independent C2 domains, showing broad binding to anionic lipids including PIP2 (Larsen & Sansom 2021). Other recent work has taken advantage of structure prediction software to clarify C2 domain folds and identify hidden domains (Dominguez et al. 2022). The approach we describe here is well suited to explore the evolutionary conservation of an electrostatic protein surface and thereby demonstrate its functional importance. These broad electrostatic surface interactions are key for binding to anionic membranes, but they are beyond the scope of co-evolution methods that have been developed for identifying evolutionarily conserved protein-protein interactions from sequence analysis (Lockless & Ranganathan 1999), or more recent learning approaches that use (in part) underlying evolutionary information to infer molecular interactions stabilizing protein complexes (Humphreys et al. 2021; Bryant et al. 2022). In general, we note that methods for learning protein-membrane interactions that integrate physical models and large-scale data sets seem to lag behind related methods used to infer protein-protein interactions.

This study represents a preliminary demonstration of the approach of investigating conserved electrostatic membrane-binding surfaces by using the Slp protein family as a starting example. While our approach combined automated sequence alignment and homology modeling with manual curation of sequences, future work could leverage recent advances in structure prediction (Jumper et al. 2021) to pursue broader comparisons of membrane binding protein

families and could conceivably be extended to unrelated proteins whose surfaces have converged on an electrostatically driven membrane binding function. In addition, future work could combine evolutionary analyses of electrostatic and hydrophobic surfaces, as both modes of nonspecific binding work together to determine the affinity of peripheral membrane proteins for their target membranes. For Slp family proteins, the electrostatic attraction of the conserved polybasic surface appears to be a major, evolutionarily conserved driver of target membrane affinity.

Methods

Slp-4 sequence search and protein net charge calculations

The human Slp-4 C2A sequence was used to search the Uniref 90 database to obtain an initial selection of 500 clustered sets of sequences using the MMseqs2 algorithm (Steinegger & Söding 2018). Any given clustered sequences with <50% sequence identity to the human Slp-4 C2A domain and/or containing uncharacterized proteins, Slp-4 alternative splicing isoforms, or other Slp family members were removed from the initial selection. To refine the sequence sets, a molecular phylogenetic tree was built and clades were manually curated with taxonomic information. Any sequences that produced unbranched lineages outside the clades were subjected to deletion. As a result, a total of 218 representative sequences from UniRef90 were retained for further analysis. Of the 218 Slp-4 sequences, 38 were class Mammalia, 60 were Aves, 14 were Reptilia, 6 were Amphibia, and 100 were Pisces. A FASTA file of these sequences along with the human reference sequence is including in the **Supporting Information**, along with a spreadsheet containing sequence ID numbers and further annotation of each sequence. A breakdown of the percent identity of each sequence versus the human Slp-4 C2A sequence is shown in **Figure S2**.

A multiple sequence alignment of the retained Slp-4 C2A domains was built using COBALT (Papadopoulos & Agarwala 2007) based on conserved domain and local sequence similarity information among the sequences. The gap penalties were set as follows: gap opening penalty of -11, gap extension penalty of -1, end gap opening penalty of -5, and end gap extension penalty of -1. C2A domains were manually curated after the multiple sequence alignment by comparison to the human sequence in the published crystal structure (PDB: 3FDW). A new phylogenetic tree for the selected Slp-4 C2A domains was constructed using the Maximum

Likelihood method in MEGA-X (version 10.1.8) with the Jones-Taylor-Thornton substitution matrix (Jones et al. 1992; Kumar et al. 2018). The Nearest-Neighbor-Interchange heuristic search (Li et al. 1996) was used for topological transformation, and the tree was bootstrapped 100 times. The tree was visualized in iToL (Letunic & Bork 2021).

Consensus sequences per taxonomic class

The consensus sequence for each vertebrate taxonomic class was determined by identifying the most abundant residue at each position. All consensus sequences were built and aligned using the AlignIO module in the Bio.Align Python package (Cock et al. 2009). The consensus sequences had the following percent identity when compared to the human Slp-4 C2A: 95% for Mammalia, 72% for Aves, 77% for Reptilia, 69% for Amphibia, and 61% for Pisces.

3D Homology Models and Electrostatic Surface Charge Calculations

The crystal structure of the human Slp-4 C2A (PDB ID: 3FDW.pdb) was used to construct the 3D homology models for the five consensus sequences of the Slp-4 C2A vertebrate classes through SWISS-MODEL (Waterhouse et al. 2018). Then the electrostatic surface charges were calculated by utilizing the webserver of APBS (Baker et al. 2001). All calculations were done at pH 7.0 and 0.15 M KCl.

Electrostatic surface charges were quantified and compared with webPIPSA (Protein Interaction Property Similarity Analysis) (Richter et al. 2008) at 300 K and 0.15 M of ionic strength. Analysis of the membrane-facing region centered on the coordinates of the sidechain CZ carbon in the phenyl ring of Phe452 in the human Slp-4 C2A crystal structure (3FDW), with a 10-Å radius from this point defining the volume of interest in each of the computed structures.

The electrostatic potential distances for each model were computed on a one-to-one basis. The distance was judged by the similarity index (SI) as computed by webPIPSA: 0 for identical, 1.4 for fully uncorrelated, and 2.0 for fully anti-correlated.

Sequence alignment of the human Slp family C2A domains

The human C2A domain sequences for Slp-1 through Slp-5 obtained through BLASTP were aligned using the Clustal Omega web service in UniProt. The similarity among residues at each position was determined by the Gonnet Point Accepted Mutation (PAM) 250 scoring matrix (Gonnet et al. 1992). Homology models and electrostatic surface charges were calculated as described above.

Conflicts of Interest

The authors declare no conflicts of interest.

Supplementary Material

Chon_etal_2023_Supporting Information.pdf: PDF file containing Figures S1-S3 and Table S1.

Chon_etal_2023_all_Slp4_sequences.fasta: FASTA file listing all Slp-4 sequence clusters analyzed.

Chon_etal_2023_Supplemental_Sequence_data.xlsx: Spreadsheet file listing all Slp-4 sequence clusters analyzed along with sequence ID number and other annotations.

Chon_etal_2023_SwissModel_structures.zip: Compressed file containing 9 homology-generated protein structure PDB files and the human Slp-4 C2A reference structure.

Acknowledgments

This work was supported by NIH grant R15GM102866. Additional support provided by the Camille and Henry Dreyfus Foundation (TH-14-028 to H.L. and TH-18-061 to J.K.) and by the CU Denver Undergraduate Research Opportunity Program to S.T.

References:

Alnaas, AA, A Watson-Siriboe, S Tran, M Negussie, JA Henderson, JR Osterberg, NL Chon, BM Harrott, J Oviedo, T Lyakhova et al. (2021) Multivalent lipid targeting by the calcium-independent C2A domain of synaptotagmin-like protein 4/granuphilin. Journal of Biological Chemistry 296. PMID: 100159 [Medline]

Baker, NA, D Sept, S Joseph, MJ Holst, JA McCammon (2001) Electrostatics of nanosystems: Application to microtubules and the ribosome. Proc Natl Acad Sci U S A 98:10037-10041. PMID: 11517324 [Medline]

Bhalla, A, MC Chicka, ER Chapman (2008) Analysis of the synaptotagmin family during reconstituted membrane fusion. Uncovering a class of inhibitory isoforms. J Biol Chem 283:21799-21807. PMID: 18508778 [Medline]

Brose, N, AG Petrenko, TC Sudhof, R Jahn (1992) Synaptotagmin: A calcium sensor on the synaptic vesicle surface. Science 256:1021-1025. PMID: 1589771 [Medline]

Bryant, P, G Pozzati, A Elofsson (2022) Improved prediction of protein-protein interactions using AlphaFold2. Nature Communications 13:1265.

Chavas, LMG, K Ihara, M Kawasaki, S Torii, T Uejima, R Kato, T Izumi, S Wakatsuki (2008) Elucidation of Rab27 recruitment by its effectors: Structure of Rab27a bound to exophilin4/Slp2-a. Structure 16:1468-1477.

Cho, W, RV Stahelin (2006) Membrane binding and subcellular targeting of C2 domains. Biochim Biophys Acta 1761:838-849. PMID: 16945584 [Medline]

Chon, NL, JR Osterberg, J Henderson, HM Khan, N Reuter, JD Knight, H Lin (2015) Membrane docking of the synaptotagmin 7 C2A domain: Computation reveals interplay between electrostatic and hydrophobic contributions. Biochemistry 54:5696-5711. PMID: 26333120 [Medline]

Cock, PJ, T Antao, JT Chang, BA Chapman, CJ Cox, A Dalke, I Friedberg, T Hamelryck, F Kauff, B Wilczynski et al. (2009) Biopython: Freely available python tools for computational molecular biology and bioinformatics. Bioinformatics 25:1422-1423. PMID: 19304878 [Medline]

Corbalan-Garcia, S, JC Gomez-Fernandez (2014) Signaling through C2 domains: More than one lipid target. Biochim Biophys Acta 1838:1536-1547. PMID: 24440424 [Medline]

Corbin, JA, JH Evans, KE Landgraf, JJ Falke (2007) Mechanism of specific membrane targeting by C2 domains: Localized pools of target lipids enhance Ca^{2+} affinity. Biochemistry 46:4322-4336. PMID: ISI:000245370400011 [Medline]

Craxton, M (2010) A manual collection of Syt, Esyt, Rph3a, Rph3al, Doc2, and Dblc2 genes from 46 metazoan genomes--an open access resource for neuroscience and evolutionary biology. BMC Genomics 11:37. PMID: 20078875 [Medline]

Dominguez, MJ, JJ McCord, RB Sutton (2022) Redefining the architecture of ferlin proteins: Insights into multi-domain protein structure and function. PLoS One 17:e0270188. PMID: 35901179 [Medline]

Edwards, AS, AC Newton (1997) Regulation of protein kinase C β_{ii} by its C2 domain. Biochemistry 36:15615-15623. PMID: 9398289 [Medline]

Farrell, A, S Thirugnanam, A Lorestani, JD Dvorin, KP Eidell, DJ Ferguson, BR Anderson-White, MT Duraisingh, GT Marth, MJ Gubbels (2012) A Doc2 protein identified by mutational profiling is essential for apicomplexan parasite exocytosis. Science 335:218-221. PMID: 22246776 [Medline]

Fukuda, M (2002) The C2A domain of synaptotagmin-like protein 3 (Slp3) is an atypical calcium-dependent phospholipid-binding machine: Comparison with the C2A domain of synaptotagmin I. Biochem J 366:681-687. PMID: 12049610 [Medline]
Fukuda, M (2013) Rab27 effectors, pleiotropic regulators in secretory pathways. Traffic 14:949-963. PMID: 23678941 [Medline]
Fukuda, M, K Mikoshiba (2001) Synaptotagmin-like protein 1-3: A novel family of C-terminal-type tandem C2 proteins. Biochem Biophys Res Commun 281:1226-1233. PMID: 11243866 [Medline]
Fukuda, M, C Saegusa, K Mikoshiba (2001) Novel splicing isoforms of synaptotagmin-like proteins 2 and 3: Identification of the Slp homology domain. Biochemical and Biophysical Research Communications 283:513-519.
Galvez-Santisteban, M, AE Rodriguez-Fraticelli, DM Bryant, S Vergarajauregui, T Yasuda, I Banon-Rodriguez, I Bernascone, A Datta, N Spivak, K Young et al. (2012) Synaptotagmin-like proteins control the formation of a single apical membrane domain in epithelial cells. Nat Cell Biol 14:838-849. PMID: 22820376 [Medline]
Gonnet, GH, MA Cohen, SA Benner (1992) Exhaustive matching of the entire protein sequence database. Science 256:1443-1445. PMID: 1604319 [Medline]
Guerrero-Valero, M, C Ferrer-Orta, J Querol-Audi, C Marin-Vicente, I Fita, JC Gomez-Fernandez, N Verdaguer, S Corbalan-Garcia (2009) Structural and mechanistic insights into the association of PKCα-C2 domain to PtdIns(4,5)P2. Proc Natl Acad Sci U S A 106:6603-6607. PMID: 19346474 [Medline]
Guillen, J, C Ferrer-Orta, M Buxaderas, D Perez-Sanchez, M Guerrero-Valero, G Luengo-Gil, J Pous, P Guerra, JC Gomez-Fernandez, N Verdaguer et al. (2013) Structural insights into the Ca^{2+} and PI(4,5)P2 binding modes of the C2 domains of rabphilin 3a and synaptotagmin 1. Proc Natl Acad Sci U S A 110:20503-20508. PMID: 24302762 [Medline]
He, J, RM Haney, M Vora, VV Verkhusha, RV Stahelin, TG Kutateladze (2008) Molecular mechanism of membrane targeting by the GRP1 PH domain. Journal of Lipid Research 49:1807-1815. PMID: ISI:000257566400022 [Medline]
Humphreys, IR, J Pei, M Baek, A Krishnakumar, I Anishchenko, S Ovchinnikov, J Zhang, TJ Ness, S Banjade, SR Bagde et al. (2021) Computed structures of core eukaryotic protein complexes. Science 374:eabm4805. PMID: 34762488 [Medline]
Izumi, T (2011) Heterogeneous modes of insulin granule exocytosis: Molecular determinants. Front Biosci 16:360-367. PMID: 21196175 [Medline]
Izumi, T (2021) In vivo roles of Rab27 and its effectors in exocytosis. Cell Struct Funct 46:79-94. PMID: 34483204 [Medline]
Izumi, T, K Kasai, H Gomi (2007) Secretory vesicle docking to the plasma membrane: Molecular mechanism and functional significance. Diabetes Obes Metab 9 Suppl 2:109-117. PMID: 17919185 [Medline]
Jones, DT, WR Taylor, JM Thornton (1992) The rapid generation of mutation data matrices from protein sequences. Comput Appl Biosci 8:275-282. PMID: 1633570 [Medline]
Jumper, J, R Evans, A Pritzel, T Green, M Figurnov, O Ronneberger, K Tunyasuvunakool, R Bates, A Žídek, A Potapenko et al. (2021) Highly accurate protein structure prediction with AlphaFold. Nature 596:583-589.

Kumar, S, G Stecher, M Li, C Knyaz, K Tamura (2018) MEGA X: Molecular evolutionary genetics analysis across computing platforms. Mol Biol Evol 35:1547-1549. PMID: 29722887 [Medline]
Kuroda, TS, M Fukuda, H Ariga, K Mikoshiba (2002) The Slp homology domain of synaptotagmin-like proteins 1-4 and Slac2 functions as a novel Rab27a binding domain. J Biol Chem 277:9212-9218. PMID: 11773082 [Medline]
Kuroda, TS, M Fukuda, H Ariga, K Mikoshiba (2002) Synaptotagmin-like protein 5: A novel Rab27a effector with C-terminal tandem C2 domains. Biochemical and Biophysical Research Communications 293:899-906.
Larsen, AH, MSP Sansom (2021) Binding of Ca^{2+}-independent C2 domains to lipid membranes: A multi-scale molecular dynamics study. Structure 29:1200-1213 e1202. PMID: 34081910 [Medline]
Lemmon, MA (2008) Membrane recognition by phospholipid-binding domains. Nat Rev Mol Cell Biol 9:99-111. PMID: 18216767 [Medline]
Letunic, I, P Bork (2021) Interactive tree of life (iTOL) v5: An online tool for phylogenetic tree display and annotation. Nucleic Acids Res 49:W293-W296. PMID: 33885785 [Medline]
Li, M, J Tromp, L Zhang (1996) On the nearest neighbour interchange distance between evolutionary trees. J Theor Biol 182:463-467. PMID: 8944893 [Medline]
Lockless, SW, R Ranganathan (1999) Evolutionarily conserved pathways of energetic connectivity in protein families. Science 286:295-299.
Lyakhova, TA, JD Knight (2014) The C2 domains of granuphilin are high-affinity sensors for plasma membrane lipids. Chem Phys Lipids 182:29-37. PMID: 24184645 [Medline]
MacDougall, DD, Z Lin, NL Chon, SL Jackman, H Lin, JD Knight, A Anantharam (2018) The high-affinity calcium sensor synaptotagmin-7 serves multiple roles in regulated exocytosis. J Gen Physiol 150:783-807. PMID: 29794152 [Medline]
Murray, D, B Honig (2002) Electrostatic control of the membrane targeting of C2 domains. Mol Cell 9:145-154. PMID: 11804593 [Medline]
Nalefski, EA, JJ Falke (1996) The C2 domain calcium-binding motif: Structural and functional diversity. Protein Sci 5:2375-2390. PMID: 8976547 [Medline]
Osterberg, JR, NL Chon, A Boo, FA Maynard, H Lin, JD Knight (2015) Membrane docking of the synaptotagmin 7 C2A domain: Electron paramagnetic resonance measurements show contributions from two membrane binding loops. Biochemistry 54:5684-5695. PMID: 26322740 [Medline]
Papadopoulos, JS, R Agarwala (2007) Cobalt: Constraint-based alignment tool for multiple protein sequences. Bioinformatics 23:1073-1079. PMID: 17332019 [Medline]
Richter, S, A Wenzel, M Stein, RR Gabdoulline, RC Wade (2008) WebPIPSA: A web server for the comparison of protein interaction properties. Nucleic Acids Res 36:W276-280. PMID: 18420653 [Medline]
Rickman, C, M Craxton, S Osborne, B Davletov (2004) Comparative analysis of tandem C2 domains from the mammalian synaptotagmin family. Biochem J 378:681-686. PMID: 14713287 [Medline]
Serano, J, GM Rubin (2003) The *Drosophila* synaptotagmin-like protein bitesize is required for growth and has mRNA localization sequences within its open reading frame. Proc Natl Acad Sci U S A 100:13368-13373. PMID: 14581614 [Medline]
Steinegger, M, J Söding (2018) Clustering huge protein sequence sets in linear time. Nature communications 9:2542. PMID: 29959318 [Medline]

Sutton, RB, BA Davletov, AM Berghuis, TC Sudhof, SR Sprang (1995) Structure of the first C2 domain of synaptotagmin I: A novel Ca^{2+}/phospholipid-binding fold. Cell 80:929-938. PMID: 7697723 [Medline]

Tellez-Arreola, JL, A Martinez-Torres, AE Flores-Moran, JM Lazaro-Guevara, A Estrada-Mondragon (2022) Analysis of the mctp amino acid sequence reveals the conservation of putative calcium- and lipid-binding pockets within the C2 domains in silico. J Mol Evol 90:271-282. PMID: 35604448 [Medline]

Tomas, A, P Meda, R Regazzi, JE Pessin, PA Halban (2008) Munc 18-1 and granuphilin collaborate during insulin granule exocytosis. Traffic 9:813-832. PMID: 18208509 [Medline]

Tsuboi, T (2009) Molecular mechanism of attachment process of dense-core vesicles to the plasma membrane in neuroendocrine cells. Neurosci Res 63:83-88. PMID: 19059288 [Medline]

van Meer, G, DR Voelker, GW Feigenson (2008) Membrane lipids: Where they are and how they behave. Nat Rev Mol Cell Biol 9:112-124. PMID: 18216768 [Medline]

Voelker, DR. Lipid assembly into cell membranes. In: Vance, DE, JE Vance, Eds. (2008) Biochemistry of lipids, lipoproteins and membranes. Elsevier, Amsterdam, pp. 441-484.

Wan, C, B Wu, Z Song, J Zhang, H Chu, A Wang, Q Liu, Y Shi, G Li, J Wang (2015) Insights into the molecular recognition of the granuphilin C2A domain with PI(4,5)P2. Chem Phys Lipids 186:61-67. PMID: 25595293 [Medline]

Wang, J, T Takeuchi, H Yokota, T Izumi (1999) Novel rabphilin-3-like protein associates with insulin-containing granules in pancreatic beta cells. J Biol Chem 274:28542-28548. PMID: 10497219 [Medline]

Waterhouse, A, M Bertoni, S Bienert, G Studer, G Tauriello, R Gumienny, FT Heer, TAP de Beer, C Rempfer, L Bordoli et al. (2018) Swiss-model: Homology modelling of protein structures and complexes. Nucleic Acids Res 46:W296-W303. PMID: 29788355 [Medline]

Yamaoka, M, T Ishizaki, T Kimura (2015) Interplay between Rab27a effectors in pancreatic beta-cells. World J Diabetes 6:508-516. PMID: 25897360 [Medline]

Yi, Z, H Yokota, S Torii, T Aoki, M Hosaka, S Zhao, K Takata, T Takeuchi, T Izumi (2002) The Rab27a/granuphilin complex regulates the exocytosis of insulin-containing dense-core granules. Mol Cell Biol 22:1858-1867. PMID: 11865063 [Medline]

Yu, M, K Kasai, K Nagashima, S Torii, H Yokota-Hashimoto, K Okamoto, T Takeuchi, H Gomi, T Izumi (2007) Exophilin4/Slp2-a targets glucagon granules to the plasma membrane through unique Ca^{2+}-inhibitory phospholipid-binding activity of the C2A domain. Mol Biol Cell 18:688-696. PMID: 17182843 [Medline]

Zhang, D, L Aravind (2010) Identification of novel families and classification of the C2 domain superfamily elucidate the origin and evolution of membrane targeting activities in eukaryotes. Gene 469:18-30. PMID: 20713135 [Medline]

Zhang, D, L Aravind (2012) Novel transglutaminase-like peptidase and C2 domains elucidate the structure, biogenesis and evolution of the ciliary compartment. Cell Cycle 11:3861-3875. PMID: 22983010 [Medline]

Zhang, X, J Rizo, TC Sudhof (1998) Mechanism of phospholipid binding by the C2A-domain of synaptotagmin I. Biochemistry 37:12395-12403. PMID: 9730811 [Medline]

Figures and legends

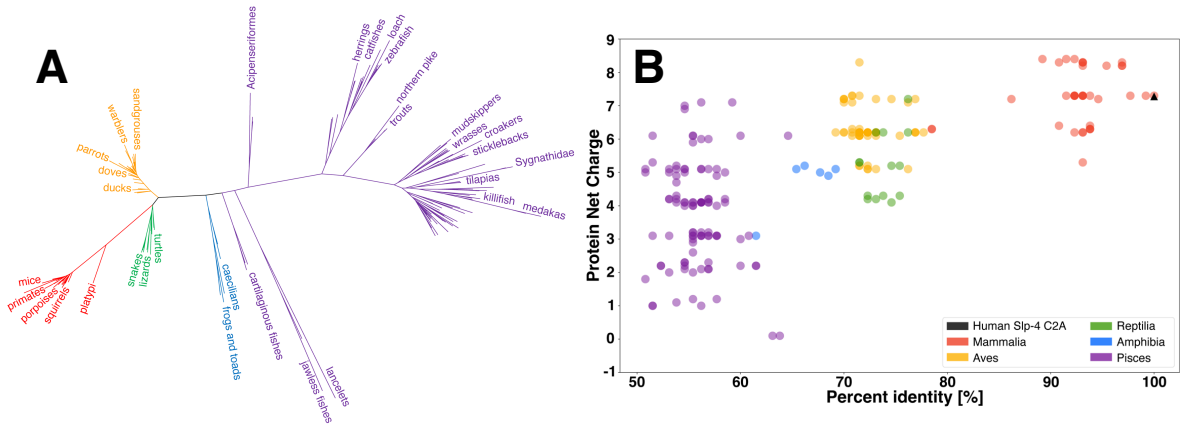

Figure 1. Sequence and net charge comparisons. A: A phylogenetic tree of Slp-4 C2A sequences used in this study. **B:** Correlation between the C2A domain net charge and percent identity relative to the human sequence. Colors reflect taxonomic class: Mammalia in red, Aves in yellow, Reptilia in green, Amphibia in blue, and Pisces in purple. A fully annotated version of panel A can be found in the Supporting Information, **Figure S3**.

```
                  354   360        370        380        390        400
Human Slp-4 C2A     IFVTGRI AFSLKYEQQT QSLVVHVKEC HQLAYADEAK KRSNPYVKTY
       Mammalia     IFVTGKI AFSLKYEQQT QTLVIHVKEC HQLAYADEAK KRSNPYVKTY
           Aves     VAVTGGI SFSLSYEQKT QTLFIHVKEC RQLAYGDEGK KRSNPYVKTY
       Reptilia     VCVTGEI AFSLSYEEKT QALFIHVKEC RHLAYADEAK KRSNPYVKTY
       Amphibia     VIVTGEI IFSLKYD/KT QILSIHVKEC RNLAYGDDAK RRSNPYVKSY
         Pisces     VEVSGDI VFSLSYDEHT QSLQVFIKEC HGLAYGDASR QLSNPYVKCY
                    : *:* *  ***.*: :* * * :.:*** : ***.* .: : ****** *
                        410        420        430        440        450
Human Slp-4 C2A LLPDKSRQGK RKTSIKRDTV NPLYDETLRY EIPESLLAQR TLQFSVWHHG
       Mammalia LLPDKSRQGK RKTSIKRDTI NPLYDEILRY EIPESLLAQR TLQFSVWHHG
           Aves LLPDKSRQGK RKTTIKRNTI NPLYNELLKY EINKSLLLAR TLQFSVWHHD
       Reptilia LLPDKSRQGK RKTTIKRNTV NPLYNELLKY EINKSLLLTR TLQFSVWHHD
       Amphibia LLPDKSRQGK RKTTIKRNTV NPLYNEVL/Y I/PESVLL/R TLQLSVWHHD
         Pisces LLPDKSRQSK RKTSIKRNTV NPVYNETLKY SISRSQLFTR SLLISVWHHG
                ********.* ***:***:*: **:*:* *:*  : .* *  * :* :*****.
                        460        470        480 483
Human Slp-4 C2A RFGRNTFLGE AEIQMDSWKL DKKLDHCLPL HGK
       Mammalia RFGRNTFLGE AEVQMDSWKL DKKLDHCLPL HGK
           Aves RFGRNTFLGE VEVPLDAWNF ESHLEEFLPL HGK
       Reptilia RFGRNTFLGE VEVPMDSWNF ESQLEECLPL HGK
       Amphibia RFGRNTFLGE VNLPLDSWNF DSQMEECLPL HGK
         Pisces RLSRNAFLGE VEIPLDCRDL DSPHEECVAL MGK
                *:.**:**** .:: :*. .: :.  :. : *  **
```

Figure 2: Slp-4 C2A comparison of primary consensus sequences by taxonomic class. Red boxes indicate the consensus sequence for PIP_2 binding (Guerrero-Valero et al. 2009; Corbalan-Garcia & Gomez-Fernandez 2014), which is completely conserved. Residues in blue boxes are additional ones that made significant contact with anionic lipids in our molecular dynamics simulations of human Slp-4 C2A (Alnaas et al. 2021). Blue text shows residues conserved as K or R; purple text shows residues conserved as basic. Symbols underneath the sequences illustrate the overall level of conservation for each residue: completely conserved (*), strongly similar (:), weakly similar (.). In Amphibia, forward-slashes (/) indicate positions at which two or more residues were equally common among the six sequence clusters: at position 368, Gly (2), His (2) and Ala (2) were found equally; at position 429, Lys (3) and Gln (3); at position 432, Val (3) and Ile (3); at position 439, Val (2) and Ser (2).

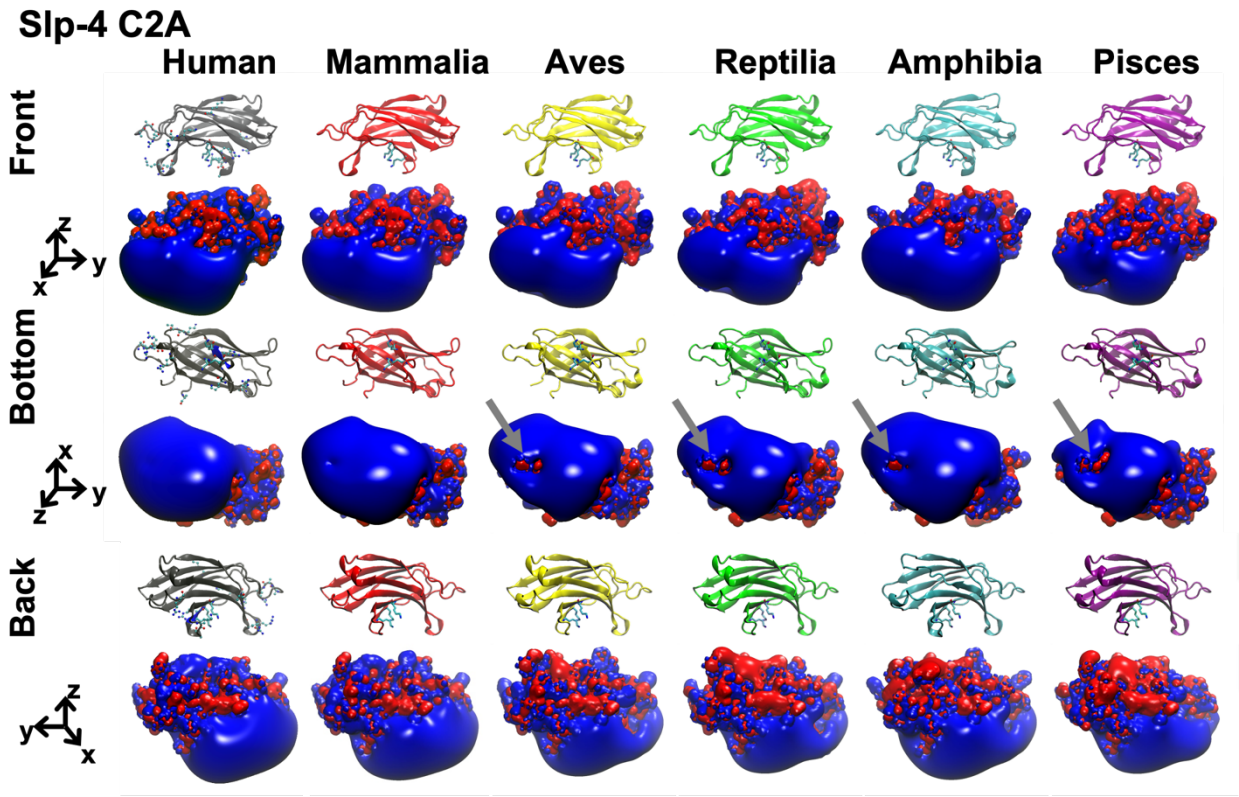

Figure 3. Electrostatic surfaces of Slp-4 C2A domain consensus structures. The homology model structures and electrostatic surface charge maps are shown for the five consensus sequences of Mammalia (red), Aves (yellow), Reptilia (green), Amphibia (blue), and Pisces (purple) with the crystal structure of the human Slp-4 C2A (gray). In the electrostatic surfaces, red represents negative charge potential (-3.5 eV) while blue represents positive charge potential (+3.5 eV). Gray arrows indicate partial negative charge near the hydrophobic Phe452.

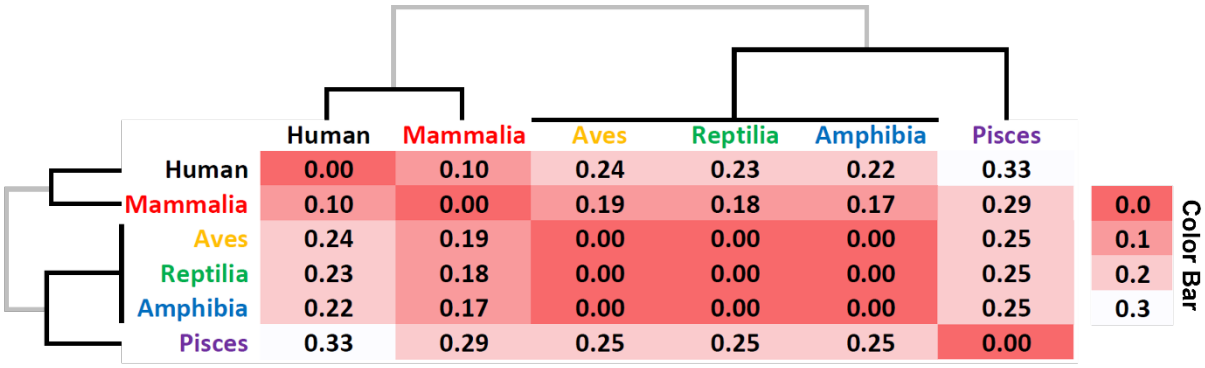

	Human	Mammalia	Aves	Reptilia	Amphibia	Pisces
Human	0.00	0.10	0.24	0.23	0.22	0.33
Mammalia	0.10	0.00	0.19	0.18	0.17	0.29
Aves	0.24	0.19	0.00	0.00	0.00	0.25
Reptilia	0.23	0.18	0.00	0.00	0.00	0.25
Amphibia	0.22	0.17	0.00	0.00	0.00	0.25
Pisces	0.33	0.29	0.25	0.25	0.25	0.00

Figure 4. **Quantitative comparison of electrostatic surface charge in Slp-4 C2A homology model structures.** Comparison values were calculated using webPIPSA for a sphere of 10-Å radius centered on the coordinates of Phe452 in the crystal structure of the human Slp-4 C2A. Smaller values represent more similar electrostatic surface charge profiles. A dendrogram tree shows the correlations between the models. The matrix is symmetrical.

```
                  354   360        370        380        390        400
Human Slp-4 C2A     IFVTGRI AFSLKYEQQT QSLVVHVKEC HQLAYADEAK KRSNPYVKTY
Human Slp-1 C2A     VQVRGSV HFALHYEPGA AELRVHVIQC QGLAAA--RR RRSDPYVKSY
Human Slp-2 C2A     LEVKGNI QFAIEYVESL KELHVFVAQC KDLAAADVKK QRSDPYVKAY
Human Slp-3 C2A     ANVTGEI EFAIHYCFKT HSLEICIKAC KNLAYGEEKK KKCNPYVKTY
Human Slp-5 C2A     VKVSGEI LLHISYCYKT GGLYIFVKNC RNLAIGDEKK QRTDAYVKSY
                      * * :  : : *       * : :  * : ** .   : :: : ***:*
                         410        420        430        440        450
Human Slp-4 C2A LLPDKSRQGK RKTSIKRDTV NPLYDETLRY EIPESLLAQR TLQFSVWHHG
Human Slp-1 C2A LLPDKQS--K RKTAVKKRNL NPVFNETLRY SVPQAELQGR VLSLSVWHRE
Human Slp-2 C2A LLPDKGKMGK KKTLVVKKTL NPVYNEILRY KIEKQILKTQ KLNLSIWHRD
Human Slp-3 C2A LLPDRSSQGK RKTGVQRNTV DPTFQETLKY QVAPAQLVTR QLQVSVWHLG
Human Slp-5 C2A LLPDKSRNNK RKTKIRI-GT NPEFNETLKY TISHTQLETR TLQLSVWHYD
                ****:    * :** :      :* ::* *:*  :    *  :  *..*:**
                         460        470      478      483
Human Slp-4 C2A RFGRNTFLGE AEIQMDSWKL DKKLDHCL ---PLHGK
Human Slp-1 C2A SLGRNIFLGE VEVPLDTWDW GSE----P TWLPLQPR
Human Slp-2 C2A TFKRNSFLGE VELDLETWDW DNKQNKQL RWYPLKRK
Human Slp-3 C2A TLARRVFLGE VIIPLATWDF EDSTTQSF RWHPLRAK
Human Slp-5 C2A RFGRNSFLGE VEIPFDSWNF ENPTDEWF VLQPKVEF
                 : *. **** . : : :*.   .          *
```

Figure 5: Alignment of human Slp C2A domain sequences. The top line shows the numbering of Slp-4 C2A for consistency in comparisons. Sequence ranges of other proteins shown are 626-758 in Slp-2, 267-391 in Slp-1, 304-436 in Slp-3, and 404-536 in Slp-5. Red boxes indicate the consensus sequence for PIP_2 binding (Wan et al. 2015), which is completely conserved. Residues in blue boxes are additional ones that made significant contact with anionic lipids in our molecular dynamics simulations of human Slp-4 C2A (Alnaas et al. 2021). Blue text shows residues strictly conserved; purple text shows residues conserved as basic. Symbols underneath the sequences illustrate the overall level of conservation for each residue: completely conserved (*), strongly similar (:), weakly similar (.) as defined by the Gonnet PAM 250 scoring matrix (Gonnet et al. 1992). Dashes indicate that a given residue is absent in the sequence.

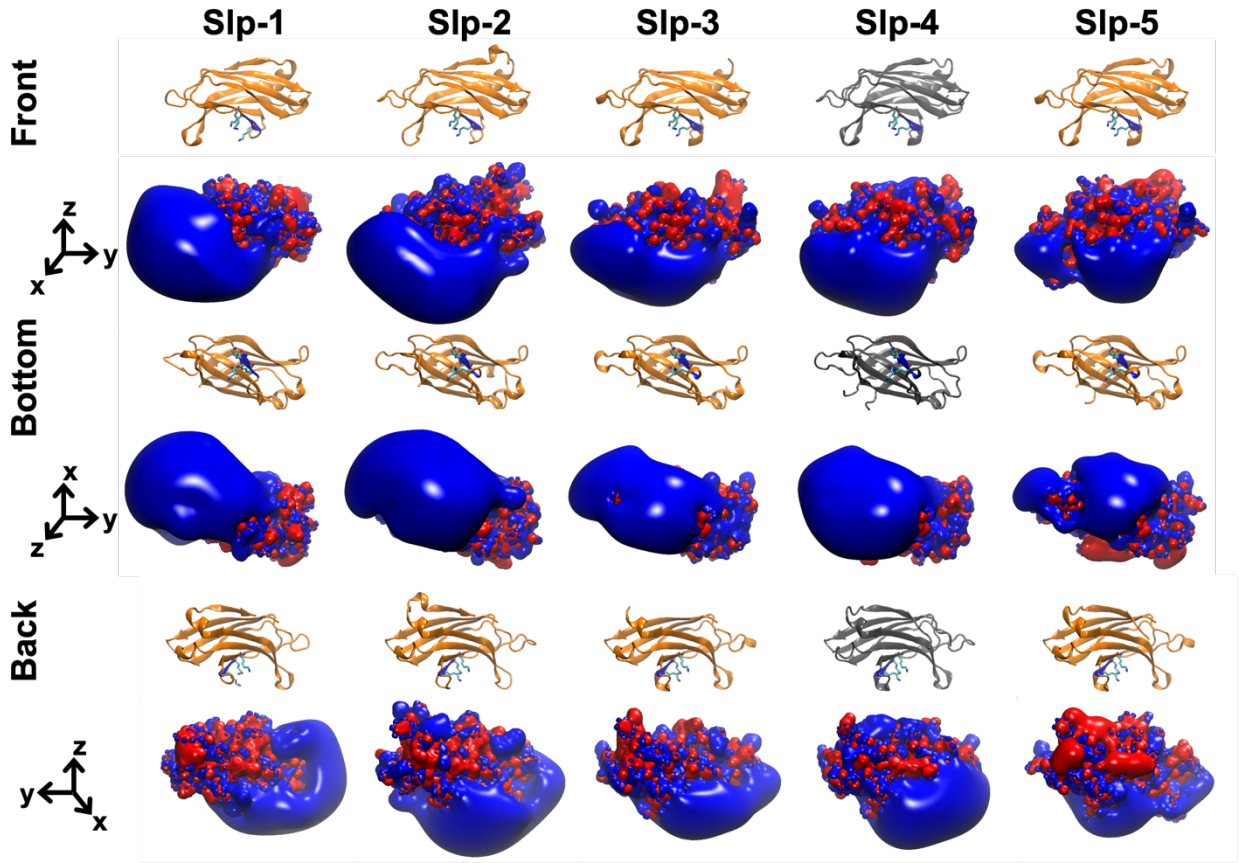

Figure 6. Electrostatic surfaces of human Slp family C2A domains. The electrostatic surface charge distributions are shown for the homology models of the C2A domains from human Slp-1, Slp-2, Slp-3, and Slp-5 along with the crystal structure of the human Slp-4 C2A domain (gray). In the electrostatic surfaces, red represents negative charge potential (-3.5 eV) while blue represents positive charge potential (+3.5 eV).

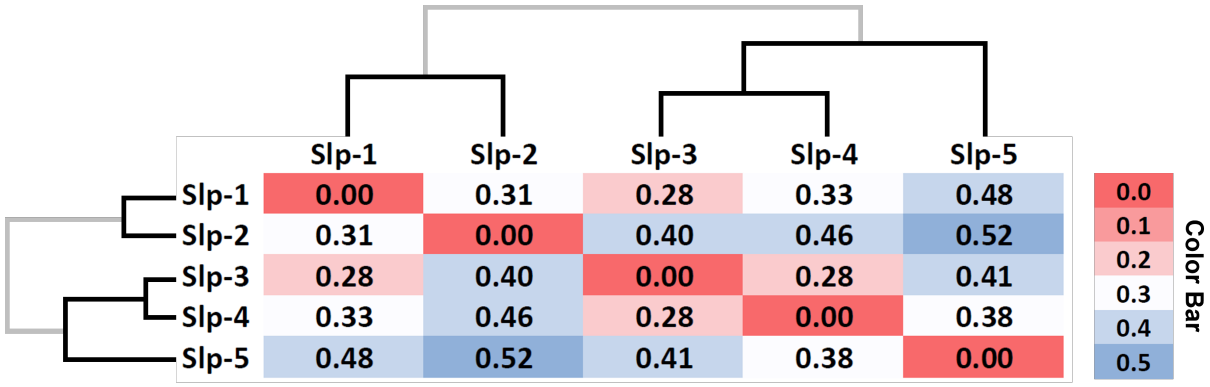

Figure 7. **Quantitative comparison of electrostatic surface charge in human Slp family C2A homology model structures.** Comparison values were calculated for each model structure using webPIPSA for a sphere of 10-Å radius centered on the coordinates of Phe452 in the human Slp-4 crystal structure. Smaller values (red) represent more similar electrostatic surface charge profiles. A dendrogram tree represents the correlations between the models.

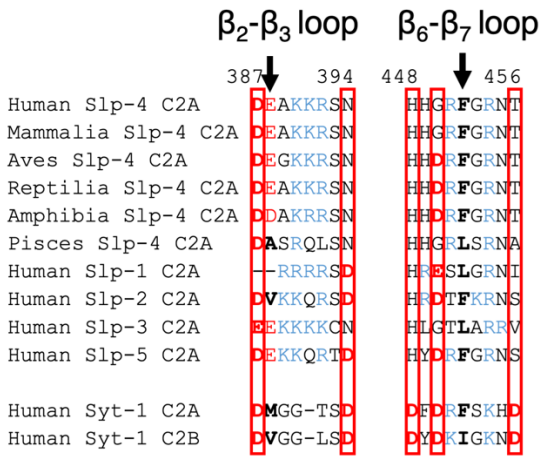

Figure 8. **Slp C2A comparison to Ca^{2+}-dependent C2 domains of synaptotagmin-1 (Syt-1).** The β_2-β_3 and β_6-β_7 loop sequences are shown (also called CBL1 and CBL3, respectively, in Ca^{2+}-dependent C2 domains). Asp and Glu residues are shown in red; Lys and Arg are shown in blue. Boxes indicate positions of conserved Asp in Ca^{2+}-binding C2 domains. Arrows indicate positions of conserved hydrophobic character in synaptotagmins; nonpolar residues at these positions are in bold.